Excitation of quasinormal ringing of a Schwarzschild black hole

Yonghe Sun and Richard H. Price
Department of Physics, University of Utah, Salt Lake City, Utah 84112
(Received 25 February 1988)

Processes near the event horizon of a black hole excite a ringing of fields (electromagnetic, gravitational perturbation, etc.) at certain complex frequencies, called quasinormal frequencies, characteristic of the hole. Evidence for such oscillations consists almost entirely of their appearance in detailed numerical solutions of specific problems. Despite the importance of quasinormal ringing in the generation of gravitational radiation, little work has been done on clarifying the way in which the ringing is excited, or in estimating the strength of the excitation, without a detailed computer solution. We formulate here the theory of the excitation of ringing of Schwarzschild holes from Cauchy data, in which a coefficient C_q seems to describe the excitation, but is given by a formally divergent integral. The meaning of C_q is shown actually to be an analytic continuation of the integral in the complex frequency plane, and this idea is used as the basis of computational techniques for finding C_q. We then demonstrate that C_q does not in general describe the astrophysically interesting quantity, the near-horizon stimulation of the ringing. We introduce two approaches to the correct description. The first uses a modified C_q based on an *ad hoc* modification of the Cauchy data. The second is based on a series representation of C_q; a truncation of this series automatically selects the astrophysically interesting part of C_q.

I. INTRODUCTION

One of the most interesting aspects of gravitational-wave detection will be the connection with black holes. Black-hole processes may provide the best detectable source of gravitational radiation and gravitational radiation may provide the best way of studying holes. In particular, black-hole radiation exhibits certain frequencies characteristic of the parameters of the hole and independent of the process giving rise to the radiation. These "quasinormal" (QN) frequencies should appear, in principle, in the electromagnetic radiation produced near a hole, but the frequencies, 10^5 Hz or less, are too low to propagate in an astrophysical environment. Low-frequency gravitational waves *can* propagate and it is at low frequencies that searches for gravitational waves will be carried out.[1]

QN frequencies arise theoretically as the complex frequencies at which source-free perturbations (electromagnetic, gravitational, etc.) of a black-hole spacetime propagate inward at the horizon, and outward at spatial infinity. Since these are the physically correct boundary conditions on the evolution of any perturbation field of a hole, it is reasonable to expect that some evidence of these special frequencies will show up in the resulting radiation. QN oscillations were first noticed by Vishveshwara[2] in calculations of the scattering of gravitational waves by a Schwarzschild black hole. Press[3] soon after coined the term quasinormal frequencies. QN oscillations have been found in perturbation calculations of particles falling into Schwarzschild holes,[4] of gravitational disturbances of rapidly rotating Kerr holes,[5] and of the collapse of a rotating star to form a Kerr hole.[6–8] Numerical investigations of the fully nonlinear equations of general relativity have given results qualitatively similar to the results of perturbation calculations. In particular, numerical studies of head-on collision of two black holes,[9] and of gravitational collapse to form a Kerr hole,[10] have produced gravitational radiation dominated by QN oscillations.

Various approaches have been given to the computation of QN frequencies,[3,11–15] but relatively little attention has been given to understanding what details of a perturbation determine the strength with which QN ringing of a black-hole spacetime is excited. Cunningham, Price, and Moncrief[6–8] gave an *ad hoc* rule for the QN energy in the gravitational radiation from a collapsing star. Leaver[16] has presented analytic and numerical results related to the present paper. Aside from these two investigations there seem to be no studies of the principles of QN mode excitation. Most important, there is no useful way of estimating the energy of QN gravitational waves from astrophysical sources, or of understanding what features of a problem determine the strength of the QN ringing it leads to. We attempt here to lay the groundwork for understanding these issues.

The mathematics of the QN modes of the spacetime will be seen to have a superficial resemblance to the mathematics of the normal modes of a linear system governed by a self-adjoint operator. The linear operator which determines QN modes is not self-adjoint (due to the QN boundary conditions) and QN modes differ from normal modes in important mathematical details: the QN frequencies are complex, the QN modes do not form a complete set, etc. The most crucial difference, however, is a qualitative one: The mathematical procedure for determining the excitation of a normal mode is clear, definitive, and straightforward. For QN modes the very meaning of the strength of the excitation can be vague.

In this paper we will limit considerations to

 ©1988 The American Physical Society

Schwarzschild black holes, and to QN ringing of a perturbation field which is specified with Cauchy data on a spacelike hypersurface. The latter is a serious limitation; for problems involving collapse of a star to form a hole, boundary data would involve Dirichlet data on the surface of the collapsing star, a timelike surface. The generalization of the present work to other boundary conditions will be given in a future paper.

We start, in Sec. II, by defining an excitation coefficient C_q for the QN ringing. The formal result is an integral over radius, which in general diverges. It is shown that the formally divergent integral must be interpreted as an analytic continuation, in the complex frequency plane, from frequencies at which the integral converges to QN frequencies. This interpretation is used in Sec. III where specific techniques are presented for accomplishing the analytic continuation. In Sec. IV we show that the coefficient C_q does *not* in general give a meaningful measure of the extent to which QN energy is present in radiation. The flaw in C_q is that it is too sensitive to Cauchy data far from the horizon, whereas QN ringing is primarily excited by perturbations fairly close to the horizon. An *ad hoc* method of modifying the Cauchy data is presented which gives useful results. An alternate approach to a useful answer for QN energy is given in which the excitation coefficient C_q is represented as an expansion. If only a few terms in that expansion are kept, the excess influence on C_q of distant Cauchy data is eliminated.

The conventions and notations used in the paper are generally those of Misner, Thorne, and Wheeler.[17] For special notations dealing with quasinormal mode excitations we will use notation similar, but not identical, to that of Leaver.[16]

II. THEORY OF THE EXCITATION COEFFICIENT C_q

A. Excitation of quasinormal ringing

The Schwarzschild spacetime background is described with the line element

$$ds^2=-(1-1/r)dt^2+(1-1/r)^{-1}dr^2 +r^2(d\theta^2+\sin^2\theta\, d\phi^2)\ , \tag{2.1}$$

where we are using units in which $c=G=2M=1$. It is useful to introduce an auxiliary coordinate x (r_* in the notation of Leaver[16] and of Misner, Thorne, and Wheeler[17]) defined by

$$x=r+\ln(r-1)\ , \tag{2.2}$$

and ranging from $x=-\infty$ (the horizon) to $x=+\infty$ (spatial infinity). Perturbations on the spacetime are decomposed into multipole moments as $\sum_{lm}\Psi_{lm}(x,t)Y_{lm}(\theta,\phi)$, where the functions $\Psi_{lm}(x,t)$ satisfy

$$\frac{\partial^2\Psi_{lm}}{\partial x^2}-\frac{\partial^2\Psi_{lm}}{\partial t^2}-V(x)\Psi_{lm}=0\ . \tag{2.3}$$

The potential $V(x)$ has the form

$$V(x)=\frac{r-1}{r^3}\left[l(l+1)-\frac{\sigma^2-1}{r}\right]\ , \tag{2.4}$$

with σ taking the value 0, 1, and 2, respectively for scalar, electromagnetic, and gravitational perturbations. For simplicity we shall henceforth omit the multipole indices. The origins of these equations are reviewed by Leaver.[16] Much of the discussion of the excitation of QN ringing, and of the C_q coefficient, will not depend on the detailed form of $V(x)$, but only on the fact that it dies off at $|x|\to\pm\infty$.

For the present we assume that the auxiliary data for Eq. (2.3) are Cauchy data, Ψ and $\partial\Psi/\partial t$, on the initial surface $t=0$. We assume that $\Psi(x,t)$ is well behaved at $t\to\infty$ and we define the Laplace transform $\psi(x,s)$ by

$$\mathcal{L}[\Psi(x,t)]=\psi(x,s)=\int_0^\infty e^{-st}\Psi(x,t)dt\ , \tag{2.5a}$$

$$\Psi(x,t)=\frac{1}{2\pi i}\int_\Gamma e^{st}\psi(x,s)ds\ , \tag{2.5b}$$

where Γ is a vertical contour in the right half of the complex s plane. From the usual properties of the Laplace transform, in particular $\mathcal{L}(\partial\Psi/\partial t)=-\Psi(x,t=0)+s\psi(x,s)$, the transformed version of Eq. (2.3) is found to be

$$\frac{\partial^2\psi}{\partial x^2}-[s^2+V(x)]\psi=S(x,s) =-s\Psi\,|_{t=0}-\left.\frac{\partial\Psi}{\partial t}\right|_{t=0}\ . \tag{2.6}$$

Since $V(x)\to 0$ as $|x|\to\infty$ the homogeneous solutions to Eq. (2.6) will have the asymptotic form $e^{\pm sx}$. We define two special independent homogeneous solutions $y_L(x,s)$ and $y_R(x,s)$ by their asymptotic behaviors

$$y_L\underset{x\to-\infty}{\sim}e^{sx},\quad y_R\underset{x\to+\infty}{\sim}e^{-sx}\ . \tag{2.7}$$

(These correspond, respectively, to the functions ψ_{r+} and $\psi_{\infty+}$ of Leaver.[16]) Since we will need these definitions to apply for arbitrary complex s some care must be taken with their definition. More specifically y_L, as a function of r, has the form $(r-1)^s$ multiplied by a function of r which is analytic[13] near $r=1$ for all s. The precise nature of the asymptotic behavior of y_R is best discussed with Leaver's expansion in terms of spheroidal wave functions.[16] At the opposite limits these functions have the forms

$$\begin{aligned} y_L&\underset{x\to+\infty}{\sim}A_{\rm in}(s)e^{sx}+A_{\rm out}(s)e^{-sx}\ ,\\ y_R&\underset{x\to-\infty}{\sim}B_{\rm in}(s)e^{sx}+B_{\rm out}(s)e^{-sx}\ . \end{aligned} \tag{2.8}$$

The Wronskian of the two solutions is

$$W(s)\equiv y_L\frac{dy_R}{dx}-y_R\frac{dy_L}{dx} =-2sA_{\rm in}(s)=-2sB_{\rm out}(s)\ . \tag{2.9}$$

The QN values s_q of s are the values for which

$$A_{\text{in}}(s_q)=B_{\text{out}}(s_q)=0\ . \tag{2.10}$$

At these values of s, y_L and y_R are not independent but are related by

$$\begin{aligned} y_L(x,s_q)&=A_{\text{out}}(s_q)y_R(x,s_q)\\ &=y_R(x,s_q)/B_{\text{in}}(s_q)\ . \end{aligned} \tag{2.11}$$

Since $V(x)$ is real in Eq. (2.6) the solutions s_q of Eq. (2.10) must occur in complex conjugate pairs s_q and s_q^*. When we speak of excitation of a QN mode we will in general mean excitation of a conjugate pair. Accurate and extensive tables of s_q have been given by Leaver.[13] Quasinormal frequencies correspond to waves moving outward at spatial infinity and inward at the horizon, the boundary conditions that must apply to any physically acceptable perturbation field. The solution to Eq. (2.6) with these boundary conditions can be shown by standard techniques to be given by

$$\psi(x,s)=\frac{1}{W(s)}\left[y_R(x,s)\int_{-\infty}^{x}y_L(x',s)S(x',s)dx' +y_L(x,s)\int_{x}^{\infty}y_R(x',s)S(x',s)dx'\right]\ . \tag{2.12}$$

We characterize the intensity of the QN excitation at frequency s_q with the excitation coefficient C_q, such that the QN ringing in $\Psi(x,t)$, at s_q, can be written as

$$\Psi(x,t)\,|_{s_q}=C_q y_R(x,s_q)e^{s_q t}\ . \tag{2.13}$$

For $x\gg 1$, that is, for a radius very large compared to the horizon radius, $y_R\approx e^{-s_q x}$ and Ψ has the form $C_q e^{s_q(t-x)}$. The appearance of QN ringing is associated with a singularity in $\psi(x,s)$ at $s=s_q$, and the singular behavior originates from the zeros of $W(s)$. We follow Leaver's notation[16] and approximate $W(s)$ by

$$W(s)=2s_q(s-s_q)\alpha_q+O((s-s_q)^2) \tag{2.14}$$

near $s=s_q$. It follows from Eqs. (2.11)–(2.14) that near $s=s_q$ we have

$$\psi(x,s)\approx[2s_q(s-s_q)\alpha_q]^{-1}y_R(x,s_q)\times\int_{-\infty}^{+\infty}y_L(x',s_q)S(x',s_q)dx'\ , \tag{2.15}$$

and that the excitation coefficient is given by

$$C_q=\frac{1}{2s_q\alpha_q}\int_{-\infty}^{+\infty}y_L(x,s_q)S(x,s_q)dx\ . \tag{2.16}$$

There is a serious difficulty with Eq. (2.16). For the perturbation fields to be stable all s_q must be (and all s_q are, in fact) in the left half plane (LHP) of complex s. This means that $y_L(x,s_q)$ diverges exponentially both for $x\to-\infty$ and for $x\to+\infty$. The integral exists only if the source function S is zero outside some finite range of x, or if S falls off exponentially with e-folding length $<1/\text{Re}(-s_q)$, as $|x|\to\infty$.

B. Numerical results for initial data of a finite extent

For conditions on $S(x,s)$ for which the integral exists, the expression in Eq. (2.16) does indeed give the correct value for C_q. Figure 1 shows the solution to Eq. (2.3) for Cauchy data which vanish except for $2<r<4$ where $\partial\psi/\partial t=0$ and $\psi=1+\cos[(r-3)\pi]$. This solution was found by using a second-order finite difference method, along the characteristics $t\pm x=\text{const}$, to solve the partial differential equation. Standard numerical tests have shown this numerical approach to be highly accurate. Henceforth we shall refer to this method as "numerical evolution" of the initial data. The method gives us a definitive way of assessing the validity and accuracy of our analytic approach to the evaluation of C_q.

In Fig. 1, Ψ is shown as a function of t at $r=r_0=11$ (or, equivalently, at $x=x_0=13.303$) for $l=2$ gravitational perturbations. There is a clear indication that QN ringing dominates the waveform for $t-x$ greater than about 5. For large values of $t-x$ we can match the computed Ψ very well with the functional form $Ke^{-at}\cos\omega(t-t_0)$. If we denote by s_{q1} the least damped of the s_q for $l=2$ gravitational perturbations, then the QN ringing associated with this frequency and its complex conjugate is

$$\begin{aligned}\Psi(x,t)&=C_{q1}y_R(x,s_{q1})e^{s_{q1}t}+[C_{q1}y_R(x,s_{q1})]^*e^{s_{q1}^*t}\\ &=2\,\text{Re}[C_{q1}y_R(x,s_{q1})e^{s_{q1}t}]\ .\end{aligned} \tag{2.17}$$

The four parameters K,a,ω,t_0 of the numerically evolved waveform can be compared with the two complex constants, C_{q1} and s_{q1} in Eq. (2.17). In particular, in this way we were able to estimate to three significant figures both the real and the imaginary part of C_{q1} for the excitation of the least damped $l=2$ gravitational QN mode in Fig. 1. This estimate is in excellent agreement with the result,

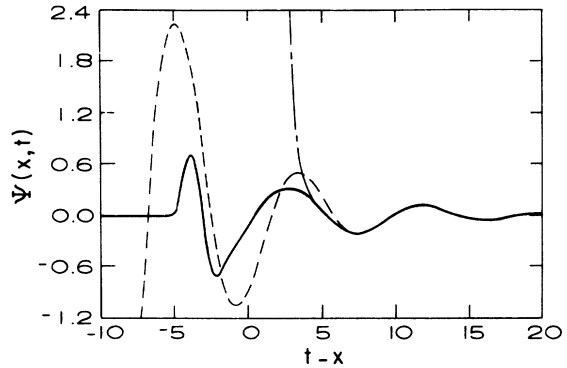

FIG. 1. Waveforms for $l=2$ gravitational perturbations resulting from Cauchy data which vanish outside a bounded interval. The initial conditions at $t=0$ are that $\partial\Psi/\partial t=0$, and that $\Psi=0$ except for $2<r<4$ where $\Psi=1+\cos[(r-3)\pi]$. The solid curve is the result of numerically evolving the data; the dashed curve shows the least-damped QN mode with the excitation coefficient computed from the formal integral expression; the curve with dashes and dots shows the superposition of the six least-damped modes. All curves are at $r=11$.

$C_{q1}=-0.377\,02+i0.329\,95$, of numerical integration of Eq. (2.16). Figure 1 shows the agreement between the numerically evolved waveform and a pure QN mode at s_{q1} with C_{q1} computed from Eq. (2.16). Shown also is the sum of the six least-damped QN modes, each with its excitation coefficient computed from Eq. (2.16). Aside from the initial turn on of the oscillations the numerically evolved waveform is extremely well described by either QN waveform, and is clearly dominated by the least-damped QN mode. A considerable number of model calculations was studied with a considerable variety of initial data. In all cases it was found that whenever the integral in Eq. (2.16) exists, its value accurately predicts the excitation.

C. C_q as an analytic continuation

In general the integral in Eq. (2.16) diverges. To understand the meaning of Eq. (2.16) we must go back to the definition, Eq. (2.5), of the Laplace transform. For Ψ well behaved as $t\to\infty$, the transform $\psi(x,s)$ will be analytic in the right half plane (RHP) of s, and only values in the RHP are needed to do the inversion in Eq. (2.5b). In principle then, $\psi(x,s)$, as given by Eq. (2.12), is defined only in the RHP. The meaning of $\psi(x,s)$ in the LHP is the analytic continuation of this $\psi(x,s)$ to the LHP. Following Leaver[16] we will assume that the analytically extended $\psi(x,s)$ has a branch point in the finite s plane only at $s=0$, so that the only specification needed for the path of analytic continuation is the way the path goes around $s=0$. Note that the s dependence of $S(x,s)$ in Eq. (2.6) is linear, so any multivalued behavior of $\psi(x,s)$ must originate in the s dependence of y_L and y_R, and will be independent of the Cauchy data. (This conclusion remains true when the initial hypersurface is more general than $t=0$. See Sec. II D below.)

To make sense of Eq. (2.16) we must take it to be the analytic continuation of some function of s which is well behaved in the s plane. The obvious guess

$$f(s)=\frac{1}{2s\alpha_q}\int_{-\infty}^{+\infty}y_L(x,s)S(x,s)dx \tag{2.18}$$

cannot be used since y_L has a part that goes as $A_{\rm in}(s)e^{sx}$ as $x\to+\infty$ [Eq. (2.8)] and therefore, for s in the RHP, the integrand in Eq. (2.18) will in general diverge as $x\to+\infty$.

To find a valid approach to treating C_q as an analytic continuation we start by defining $y_{\infty-}$ ($\psi_{\infty-}$ in the notation of Leaver[16]), a new homogeneous solution to Eq. (2.6) defined by the boundary condition

$$y_{\infty-}(x,s)\underset{x\to+\infty}{\sim}e^{sx}\ . \tag{2.19}$$

The solutions $y_{\infty-}$, y_L, and y_R are not independent, of course. In particular the relation

$$y_L(x,s)=A_{\rm in}(s)y_{\infty-}(x,s)+A_{\rm out}(s)y_R(x,s) \tag{2.20}$$

follows from Eqs. (2.7), (2.8), and (2.19). We next take s to be in the RHP, and in Eq. (2.12), which is valid in the RHP, we substitute Eq. (2.20), to arrive at

$$\psi(x,s)=y_R(x,s)\frac{f_1(x,s)}{W(s)}+f_2(x,s)\ , \tag{2.21}$$

where

$$f_1(x,s)=\int_{-\infty}^{x}y_L(x',s)S(x',s)dx' + A_{\rm out}(s)\int_{x}^{\infty}y_R(x',s)S(x',s)dx' \tag{2.22}$$

and

$$f_2(x,s)=\frac{A_{\rm in}(s)}{W(s)}y_{\infty-}(x,s)\int_{x}^{\infty}y_R(x',s)S(x',s)dx'\ . \tag{2.23}$$

Since $A_{\rm in}(s)/W(s)=-1/2s$, the function $f_2(x,s)$ will be nonsingular at $s=s_q$. [Note that $y_{\infty-}$ cannot be singular at $s=s_q$ since $y_{\infty-}(x,s)$ is well defined for all s.] Thus only the first term on the right in Eq. (2.21) can have a singularity at $s=s_q$ corresponding to QN ringing. We note that $f_1(x,s)$ is well defined in the RHP that $W(s)\approx 2s_q(s-s_q)\alpha_q$ near $s=s_q$, and that QN ringing [the Laplace transform of Eq. (2.13)] corresponds to

$$\psi(x,s)=\frac{C_q}{s-s_q}y_R(x,s_q)\ . \tag{2.24}$$

We therefore define

$$C_q(x,s)\equiv\frac{f_1(x,s)}{2s_q\alpha_q}\ . \tag{2.25}$$

From Eqs. (2.14), (2.21), and (2.24) it follows that $C_q(x,s)$ is a correct generalization, to arbitrary s, of C_q. That is, $C_q(x,s)$ is well defined in the RHP and the analytic continuation of $C_q(x,s)$ to $s=s_q$ gives C_q.

It may seem strange that $C_q(x,s)$ is a function of x, since the excitation coefficient C_q is, by definition, independent of x. The point is that C_q is independent of x at $s=s_q$. To see this, note that

$$f_1(x_1,s)-f_1(x_2,s)=\int_{x_2}^{x_1}[y_L(x,s)-A_{\rm out}(s)y_R(x,s)]S(x,s)dx\ , \tag{2.26}$$

and [from Eq. (2.11)] that $[y_L(x,s)-A_{\rm out}(s)y_R(x,s)]$ vanishes at $s=s_q$ We could eliminate the somewhat deceptive x dependence by simply setting $x=0$ in $C_q(x,s)$, but it is useful to keep $C_q(x,s)$, as defined in Eq. (2.26), as the basis for the development, in Sec. III, of specific techniques for analytic continuation.

D. More general initial data

It is reasonably straightforward to generalize the approach outlined above to a Cauchy hypersurface other than $t=0$. For $t=t_0(x)$, a single-valued function specifying a spacelike hypersurface, we replace Eq. (2.5a) with

$$\psi(x,s)\equiv\int_{t_0(x)}^{\infty}e^{-st}\Psi(x,t)dt =\int_{-\infty}^{\infty}e^{-st}\Psi(x,t)H[t-t_0(x)]dt\ , \tag{2.27a}$$

where H is the unit step function. From the last equality

it follows that this integral transform can be inverted to give

$$\Psi(x,t)=\frac{1}{2\pi i}\int_\Gamma e^{st}\psi(x,s)ds\ , \tag{2.27b}$$

for $t>t_0(x)$. In Eq. (2.27a) we can differentiate to get

$$\begin{aligned}\partial^2\psi/\partial x^2=&\int_{t_0(x)}^{\infty}e^{-st}[\partial^2\Psi(x,t)/\partial x^2]dt\\&+e^{-st_0(x)}[(st_0'^2-t_0'')\Psi(x,t)-2t_0'\partial\Psi/\partial x\\&-t_0'^2\partial\Psi/\partial t]\,|_{t=t_0(x)}\ ,\end{aligned} \tag{2.28}$$

where a prime denotes differentiation of t_0 with respect to x. It is straightforward to use this result and Eq. (2.3) to derive a differential equation for ψ which has the same form as Eq. (2.6), but in which the source term is

$$\begin{aligned}S(x,s)=-e^{-st_0(x)}&[(s-st_0'^2+t_0'')\Psi(x,t)+2t_0'\partial\Psi/\partial x\\&+(1+t_0'^2)\partial\Psi/\partial t]\,|_{t=t_0(x)}\ .\end{aligned} \tag{2.29}$$

Numerical tests have been conducted for examples in which the initial surface $t=t_0(x)$ in the t,x plane was made up of joined line segments with slopes ±1. The result of using Eq. (2.16) for these examples was in excellent agreement with the results of numerically evolving the Cauchy data.

III. EVALUATING C_q

A. Choice of spatial variable

The demonstration, in Sec. II, that C_q is the analytic continuation of an integral expression does not automatically give us a way of finding a numerical value for C_q. In this section we present several approaches to such a calculation. The starting point for all of them is Eq. (2.25) in which $f_1(x,s)$ is defined, for s in the RHP, as the integral in Eq. (2.22), and for s in the LHP as the analytic continuation of this integral. For some purposes it is useful to rewrite Eq. (2.22) as

$$\begin{aligned}f_1(x,s)=&\int_{-\infty}^{x_1}y_L(x',s)S(x',s)dx'\\&+\int_{x_1}^{x_2}y_L(x',s)S(x',s)dx'\\&+A_{\rm out}(s)\int_{x_2}^{\infty}y_R(x's)S(x',s)dx'\ .\end{aligned} \tag{3.1}$$

The middle integral, for finite x_1 and x_2, converges for s in the LHP, so it can immediately be continued to $s=s_q$ simply by evaluating the integral at $s=s_q$. In this way the numerical details of an astrophysical model can be put into the middle integral and the contribution to C_q evaluated. The difficulties at the horizon ($x=-\infty$) and at spatial infinity ($x=+\infty$) are then confined, respectively, to the first and third integrals in Eq. (3.1) and can be dealt with separately. We can, of course, choose $x_1=x_2$ so that the middle integral disappears.

Two basic approaches will be given for evaluating C_q: (i) a series expansion in the spatial variable, for dealing with the horizon integral, and (ii) a contour deformation in the complex plane of the spatial variable. For either, the dependence of the integrand on the spatial variable is crucial, and both require that the spatial variable r be used; the x variable, so useful for visualizing QN problems, must be avoided. The reason for this is that y_L is a simple analytic function of r, as can be seen in the expansion

$$y_L=(r-1)^s r^{-2s}e^{-s(r-1)}\sum_{n=0}^{\infty}a_n(s)\left[\frac{r-1}{r}\right]^n\ . \tag{3.2}$$

The expansion coefficients are given by Leaver,[13] who shows that the series is convergent, for all finite s and finite r. The series is therefore an analytic function of r (for $r<\infty$) and the singularities of y_L at $r=0$ and 1 are those displayed in the leading factors on the right-hand side of Eq. (3.2). The function $r(x)$, the inverse Eq. (2.2), has an infinite number of branch points, at $x=i\pi\pm2ni\pi$, where $n=0,1,2,\ldots$, and y_L, as a function of complex x, would have singularities at these points. In terms of the variable r the horizon and spatial-infinity contributions to C_q are

$$I_H(r_1,s)=\frac{1}{2s_q\alpha_q}\int_1^{r_1}y_L(r,s)S(r,s)\frac{r}{r-1}dr\ , \tag{3.3a}$$

$$I_{\rm mid}(r_1,s)=\frac{1}{2s_q\alpha_q}\int_{r_1}^{r_2}y_L(r,s)S(r,s)\frac{r}{r-1}dr\ , \tag{3.3b}$$

$$I_\infty(r_2,s)=\frac{A_{\rm out}(s)}{2s_q\alpha_q}\int_{r_2}^{\infty}y_R(r,s)S(r,s)\frac{r}{r-1}dr\ , \tag{3.3c}$$

with

$$C_q=I_H+I_{\rm mid}+I_\infty\ . \tag{3.4}$$

In the remainder of this section, techinques will be given for analytically continuing these expressions from s in the RHP to s_q. The general approach will be to assume that for sufficiently small (r_1-1) and for sufficiently large r_2, the source function $S(r,s)$ can be approximated in terms of functions having simple r dependence.

B. Analytic continuation at the horizon

We assume that for $r<r_1$ the source function $S(r,s)$ can be expanded in a series of powers of $r-1$. Since y_L can be written as $(r-1)^s$ multiplied by an analytic function of $r-1$ it follows that the integrand in I_H can be written as

$$y_L(r,s)S(r,s)r/(r-1)=\sum_k B_k(s)(r-1)^{k+s}\ . \tag{3.5}$$

Every term for which $\mathrm{Re}(k+s+1)>0$ can be integrated at $r=1$. If we choose $\mathrm{Re}(s)$ large enough so that every term in Eq. (3.5) can be integrated, the term by term evaluation of Eq. (3.3a) is

$$I_H(r,s)=\frac{1}{2s_q\alpha_q}\sum_k B_k(s)\frac{(r-1)^{k+s+1}}{k+s+1}\ . \tag{3.6}$$

The analytic continuation of $I_H(r,s)$ from regions of the s plane in which $\mathrm{Re}(k+s+1)>0$ to the QN frequencies is immediate. In Eq. (3.6), s is simply replaced by s_q.

Note that Eq. (3.5) does not require that the series for $S(r,s)$ be a power series, and that S therefore be analytic at $r=1$. The values of k in Eq. (3.6) need not be integers; the source function S can have a branch point at $r=1$. The expansion for S can, in fact, be much more general than a series of powers of $r-1$. It is necessary only that S can be expanded in terms of a series of functions such that (i) the series converges in some neighborhood of $r=1$, (ii) the expansion functions, when put in the integral in Eq. (3.3a), can all be integrated for some region of the complex s plane, and (iii) the resulting integrals can easily be analytically continued to the LHP, specifically to $s=s_q$.

Analytic continuation of I_H can also be carried out via a deformation of contour in the complex r plane. We assume that the source function S is nonsingular near $r=1$ so that the integrand in Eq. (3.3a) has a branch point at $r=1$ due to the factor $(r-1)^s$ in y_L. We choose the branch cut from $r=1$ to ∞ along the positive r axis, with the phase of $(r-1)$ taken to be zero just above the branch cut. To use analytic continuation we consider the integral

$$\frac{1}{2s_q\alpha_q}\int y_L(r,s)S(r,s)\frac{r}{r-1}dr$$

on the contour shown in Fig. 2(a). For s in the RHP the infinitesimal circular segment near $r=1$ makes a negligible contribution. The segment of the contour just above the branch cut gives $I_H(r_1,s)$ while the segment just below gives $-I_H(r_1,s)$ multiplied by the phase factor $\exp(2\pi i s)$ due to the phase change in $r-1$. We conclude that

$$I_H(r_1,s)=\frac{1}{1-\exp(2\pi i s)}\frac{1}{2s_q\alpha_q}\times\int y_L(r,s)S(r,s)\frac{r}{r-1}dr\ , \tag{3.7}$$

where the contour of integration is that in Fig. 2(a), and where s is in the RHP.

We can now deform the contour to the new contour γ shown in Fig. 2(b). Since the contour has been deformed through a region in which the integrand is analytic, the value of the integrand is unchanged. But with the new contour the integral in Eq. (3.7), and hence I_H, can be evaluated for any finite value of s. The evaluation of the integral in Eq. (3.7) can be done not only in principle, but in practice, with $y_L(r,s)$ given by the expansion in Eq. (3.5). This requires that the contour remain in the region $|(r-1)/r|<1$, or equivalently $\mathrm{Re}(r)>\frac{1}{2}$, and that the source function $S(r,s)$ be analytically continuable from the real axis to the deformed contour.

As a numerical example of the near-horizon techniques above, we choose initial data corresponding to the source function

$$S(r,s)=\begin{cases}s(1.5-r), & r<1.5\ ,\\ 0, & r\geq 1.5\ ,\end{cases} \tag{3.8}$$

so that complications near $r=\infty$ are avoided. For this source function $C_q=I_H(1.5,s_q)$ is computed in two ways:

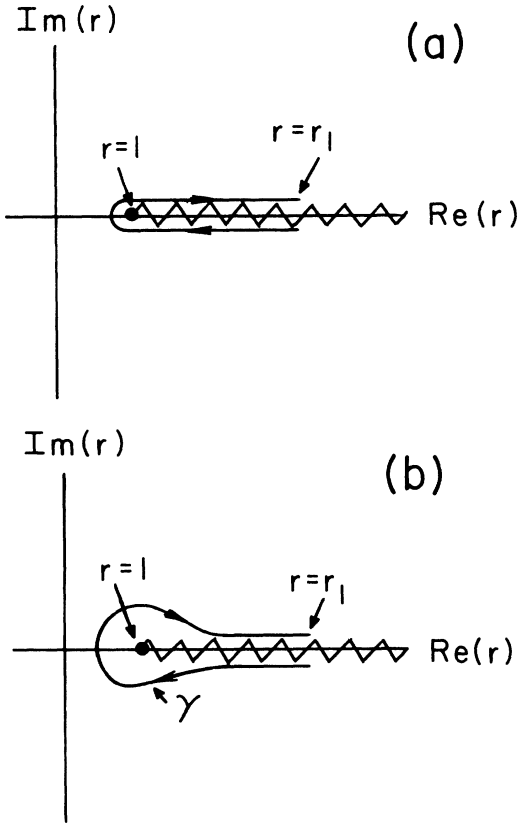

FIG. 2. Contours in the complex r plane for analytically continuing the integral $I_H(r,s)$ to QN values of s.

first by expanding the integrand in I_H in powers of $(r-1)$ and second by performing the integration in Eq. (3.7) on a contour like that shown in Fig. 2(b). For every C_q computed the two methods gave numerical results in perfect agreement (i.e., agreement at the limit of numerical precision used).

The validity of the computed values of C_q is demonstrated in Fig. 3, which shows the results of numerical evolution of the initial data in Eq. (3.8). This result is compared to the waveforms corresponding to pure QN ringing with the computed excitation coefficients, both for a single pair of QN modes, and for the superposition of six pairs of QN modes. The agreement is excellent except for very early times, at which pure QN ringing cannot give a good representation of the waveform.

C. Analytic continuation of spatial infinity

To deal with the analytic continuation of $I_\infty(r_2,s)$ we assume that the source function $S(r,s)$ can be approximated by a simple form which can be analytically continued off the real r axis. We assume furthermore that the behavior of the integrand in Eq. (3.3c) is dominated by the e^{-sr} behavior of y_R. Under these conditions analytic continuation in the complex s plane is equivalent to a contour deformation in the complex r plane.

To show this we start with a real positive value of s. The integrand in Eq. (3.3c) is then well defined. Viewed as a path in the complex r plane, the path of integration is the segment of the real axis as shown in Fig. 4. We

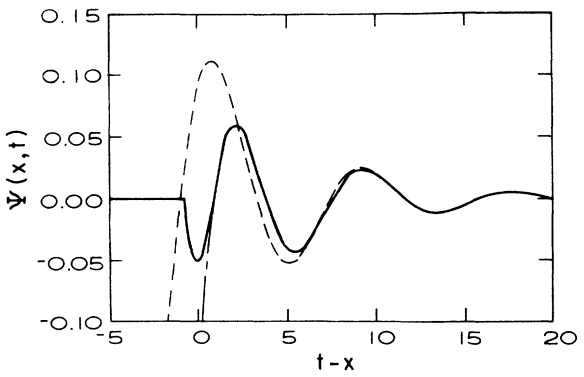

FIG. 3. Waveforms for $l=2$ gravitational perturbations from a source function that does not vanish at the horizon. The initial conditions at $t=0$ are that $\partial\Psi/\partial t=0$, and that $\Psi=0$ except that $\Psi=(r-1.5)$ for $r<1.5$. The solid curve is the result of numerically evolving the data; the dashed curve shows the least-damped QN mode with the excitation coefficient computed via a contour deformation in the complex r plane; the curve with dots and dashes shows the superposition of the six least-damped modes. All curves are at $r=11$.

can, however, deform the contour without changing the value of the integral. We must be sure that during the deformation no singularity of the integrand is crossed. The direction in which the new contour approaches infinity must also be allowable, that is, the integral must vanish along the circular arc which connects, "at infinity," the original and the new contour. For positive real s this means that the asymptotic large-$|r|$ direction of the new contour must be within 90° of the original direction. Curve Γ in Fig. 4 shows the result of a deformation which has not crossed the singularities (shown as crosses) of the integrand and which gives the same value

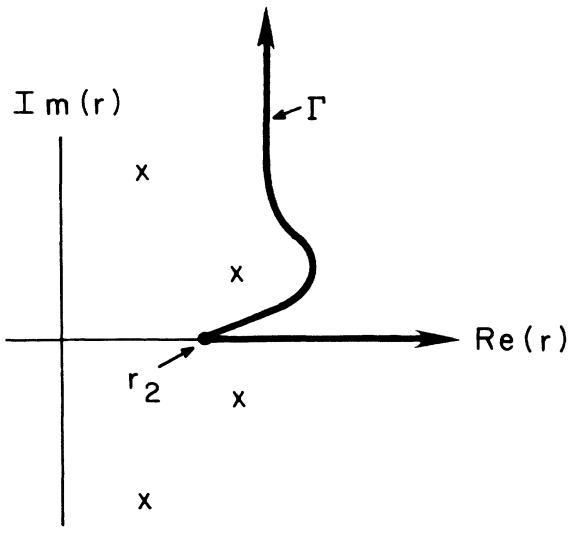

FIG. 4. Deformation of contour in the complex r plane for analytically continuing $I_\infty(r_2,s)$ to $s=s_q$. The original contour on the real r axis is rotated to contour Γ. During the rotation the contour is distorted as necessary to avoid crossing any of the singularities, shown as crosses, of the integrand in L_∞.

of $I_\infty(r_2,s)$ for real s. But for contour Γ the integral in I_∞ converges for any value of s in the lower half of the complex s plane. Contour Γ thus gives an analytic continuation of $I_\infty(r_2,s)$ to the QN frequencies in the lower half-s plane. A deformation of the original curve clockwise by 90° would give an analytic continuation to the upper half-s plane, but it is not necessary to do this. Once an excitation coefficient C_q is found for a QN frequency s_q, the coefficient for its complex conjugate s_q^* follows from $C_q(s_q^*)=[C_q(s_q)]^*$.

For a QN frequency s_q in the lower half-plane we have then the analytic continuation

$$I_\infty(r_2,s_q)=\frac{A_{\rm out}(s_q)}{2s_q\alpha_q}\int_\Gamma y_R(r,s_q)S(r,s_q)\frac{r}{r-1}dr$$

$$=\frac{1}{2s_q\alpha_q}\int_\Gamma y_L(r,s_q)S(r,s_q)\frac{r}{r-1}dr\ . \qquad (3.9)$$

The deformation of the contour and the convergence of the integral depend, of course, on the nature of $S(r,s)$. If, for example, S had the spatial dependence $\exp[-(r-1)^2]$, a rotation by, e.g., 90°, of the asymptotic direction in which the contour approaches infinity would not be valid. For this particular example rotation is unnecessary, as the integral in Eq. (3.3c) would itself converge. It is expected that for astrophysical source terms either the integral on the original path will converge for $s=s_q$ or a simple deformation, as in Fig. 4, will give an analytic continuation to $s=s_q$. It is possible, however, that some source functions will require a special choice of contour deformation.

With the last expression in Eq. (3.9) the integral can be evaluated in practice as well as in principle if the series in Eq. (3.2) is used to evaluate $y_L(r,s)$. This requires only that the deformed contour remain in the region $|(r-1)/r|<1$ [equivalently $\mathrm{Re}(r)>\frac{1}{2}$] in which the series converges. Numerical investigations of model problems confirm that this contour deformation approach gives the correct C_q, i.e., a C_q that agrees with that found by numerically evolving the initial data.

The contour deformation approach to handling the divergence at spatial infinity can be conveniently combined with the contour deformation approach used in Sec. III B to form a contour on which the integral $\int y_L S[r/(r-1)]dr$ yields C_q. The process is illustrated in Fig. 5. The choice $r_1=r_2$ is made for convenience so that $C_q=I_H(r_1,s_q)+I_\infty(r_1,s_q)$. The contour γ from Fig. 2 is used, but the branch cut is chosen to follow the path shown in Fig. 4. To γ is now added a contour Γ displaced an infinitesimal distance counterclockwise of the branch cut, as shown in Fig. 5(b). Lastly, a path Γ' parallel to Γ is added at an infinitesimal displacement clockwise of the cut, as shown in Fig. 5(c).

On γ the integral of $\int y_L S[r/(r-1)]dr$ gives

$$2s_q\alpha_q[1-\exp(2i\pi s_q)]I_H(r_1,s_q)$$

as discussed in Sec. III A. On Γ the integral gives $2s_q\alpha_q I_\infty(r_1,s_q)$. The integral on Γ' differs from that on Γ by a sign and by the factor $\exp(2i\pi s_q)$ which arises

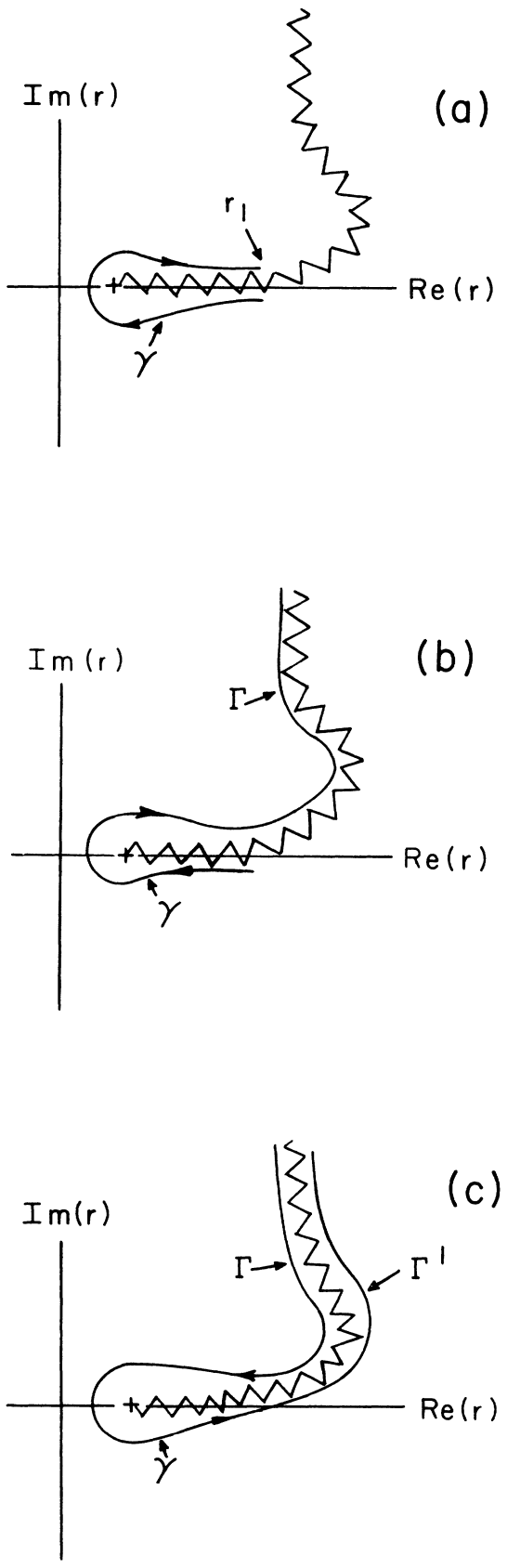

FIG. 5. The combination of the deformed contour for dealing with I_H and the deformed contour for dealing with I_∞.

from the multivalued factor $(r-1)^{s_q}$ in $y_L(r,s)$. [See Eq. (3.2).] The integral on Γ' therefore adds

$$-\exp(2i\pi s_q)2s_q\alpha_q I_\infty(r_1,s_q) .$$

When the three contributions are added together we see that[18]

$$C_q = I_H(r_1,s_q)+I_\infty(r_1,s_q)$$
$$= \frac{1}{1-\exp(2\pi i s_q)} \frac{1}{2s_q\alpha_q} \int y_L(r,s_q)S(r,s_q)\frac{r}{r-1}dr , \tag{3.10}$$

where the integral is taken on the complete contour in Fig. 5(c). Although r_1 appears in the first equality in Eq. (3.10), it is clear that r_1 has no real meaning in the final contour integration; this approach uses a single smooth contour to handle simultaneously the difficulties of the integral both at $r=1$ and at $r=\infty$.

As a check on the validity of this method, initial data were chosen to be

$$\Psi|_{t=0} = \frac{1}{(r-1.5)^2+1} ,$$
$$\partial\Psi/\partial t|_{t=0} = \frac{1}{(r-2.5)^2+4} . \tag{3.11}$$

The branch cut was chosen to be horizontal out to $r=3$ and vertically upward thereafter. The Γ and Γ' contours, infinitesimally close to the branch cut, lay to the right of the poles of S at $r=1.5+i$ and $r=2.5+2i$ so that the singularities of the integrand were not crossed as part of the contour was rotated by 90° counterclockwise from the real axis. The value of C_q computed from Eq. (3.10) with this contour agreed, within the limits of the numerical precision used, with values found by other approaches (i.e., I_H and I_∞ evaluated by separate contour deformations, or I_H evaluated by a series and I_∞ evaluated by a contour deformation). The computed values of C_q gave a waveform in excellent agreement with the numerically evolved waveform.

IV. TIMING AND THE MODIFICATION OF C_q

A. The onset of ringing

The evaluation of C_q, as presented in the preceding section, does not by itself answer the question of how much energy is radiated in the form of QN ringing. The additional crucial piece of information required is the time at which the QN ringing starts. For a given value of C_q, the earlier the start is the more energy is radiated.

Some simple arguments give an approximate idea of when QN ringing turns on: The values of the QN frequencies depend on the shape of the potential $V(x)$ in Eq. (2.4). This suggests that ringing should originate where the potential is strongest, near the peak of the potential at $x\approx 0$. At significant distances from this peak the form of the potential is simple and familiar. For $x \ll -1$ the potential vanishes, and for $x \gg 1$ the potential $V(x)$ is essentially a centrifugal potential. In neither case does

anything like QN ringing get generated; the ringing therefore must originate where $|x| \approx 1$. This conclusion is supported by a three-dimensional plot, Fig. 3 in the paper of Cunningham, Price, and Moncrief,[6] showing the development of the ringing in space and in time.

If the ringing starts near the peak of the potential, what is it that sets off the ringing? Vishveshwara studied the scattering by a black hole of an incoming gravitational waveform with a Gaussian shape $\exp(-ax^2)$. For a broad packet ($a \ll 1$) he found no QN ringing. Ringing was excited only when the width of the packet was comparable to, or smaller than unity, i.e., than the Schwarzschild radius. This suggests that Cauchy data must vary on a length scale less than or of order unity to excite ringing. This relatively rapidly varying Cauchy data, furthermore, can set off ringing only near the peak of the potential $V(x)$.

The issue of timing is closely tied to certain difficulties with the usefulness of C_q. Suppose that the Cauchy data has the form of a narrow pulse that we can approximate as a delta function $\delta(r-r_p)$. For such a pulse the integral in Eq. (2.16) does not diverge and C_q can be evaluated directly. Because of the asymptotic form $e^{-s_q x}$ of $y_L(x,s_q)$ at large x, it follows that C_q must be an exponentially increasing function of r_p. This would seem to suggest, contrary to intuition, that a bump in the Cauchy data far from the horizon will excite much more ringing than a similar bump close to the horizon. The explanation lies in timing: A bump in the Cauchy data far from the horizon must first propagate inward to the region of the potential peak before it can stimulate QN ringing. The onset of QN ringing is therefore delayed by a time $t_{\text{delay}} \approx r_p$ required for this inward propagation, and the magnitude of the ringing (e.g., the height of the first QN peak) will be suppressed by a factor of order $|\exp(s_q t_{\text{delay}})|$. This small factor will cancel the large factor $|\exp(-s_q r_p)|$ in C_q.

This phenomenon is most transparent in a model problem in which we replace the actual potential of Eq. (2.4) by a surrogate potential:[11,19]

$$V(x)=\begin{cases}0, & x<1\ ,\\ 2/x^2, & x\geq 1\ .\end{cases} \tag{4.1}$$

With this substitution the homogeneous solutions to Eq. (2.6) can be found in closed form. For $x<1$ they are simply $e^{\pm sx}$; for $x>1$ the potential is a pure dipole centrifugal barrier and the solutions are $sxh_1^{(1,2)}(sx)$, where $h_1^{(1,2)}$ represents the dipole spherical Hankel functions. By matching $y_L=e^{sx}$ for $x<1$ to $y_R=-isxh_1^{(1)}(isx)$ for $x>1$, we find that there is a single conjugate pair of QN frequencies

$$s_q=-\frac{1}{2}\pm\frac{i}{2}\ . \tag{4.2}$$

As initial data at $t=0$ for our model problem we take $\partial\Psi/\partial t=0$ and

$$\Psi(x)=\begin{cases}x/(2x_1), & 1<x_1<x<x_2\ ,\\ 0 \quad \text{otherwise}\ .\end{cases} \tag{4.3}$$

The solution for this initial data can be found in closed form and can be written as a superposition

$$\Psi(x,t)=\Psi_0(x,t)+\Psi_{\text{QN}}(x,t)\ , \tag{4.4}$$

in which Ψ_0 represents the direct propagation of the initial data and Ψ_{QN} contains the QN ringing. For $x \gg 1$ the solutions are

$$\Psi_0(x,t)=\frac{1}{4x_1}[(2x-2t-x_2)H(t-x+x_2)+(2x-2t+x_2)H(t-x-x_2+2)$$
$$-(2x-2t-x_1)H(t-x+x_1)-(2x-2t+x_1)H(t-x-x_1+2)]\ , \tag{4.5}$$

$$\Psi_{\text{QN}}(x,t)=-\frac{1}{4x_1}H(t-x-x_2+2)e^{-(t-x-x_2+2)/2}[(4-x_2)\cos\tfrac{1}{2}(t-x-x_2+2)-x_2\sin\tfrac{1}{2}(t-x-x_2+2)]$$
$$+\frac{1}{4x_1}H(t-x-x_1+2)e^{-(t-x-x_1+2)/2}[(4-x_1)\cos\tfrac{1}{2}(t-x-x_1+2)-x_1\sin\tfrac{1}{2}(t-x-x_1+2)]\ , \tag{4.6}$$

where H is the unit step function. Both in its analytic form and in the plot shown in Fig. 6, the waveform shows two distinct points at which QN ringing turns on: one point at $t=x+x_1-2$, and one at $t=x+x_2-2$. The time of the first turn on is the sum of two times: the time (x_1-1) for the sharp edge of the initial data at $x=x_1$ to propagate to the peak of the potential at $x=1$, and the time $(x-1)$ for the QN ringing to propagate from the peak of the potential out to the observation point at x. The second turn on is produced similarly by the edge of the initial data at $x=x_2$.

The excitation coefficient can be found, e.g., by a direct evaluation of Eq. (2.16). For the mode with $s_q=s_1=-0.5+i0.5$, it has the value

$$C_q=\frac{1}{8x_1}\{e^{s_1(2-x_2)}[(1-i)x_2-4]$$
$$-e^{s_1(2-x_1)}[(1-i)x_1-4]\}\ . \tag{4.7}$$

This does not seem compatible with the analytical or the graphical form of the solution. As x_2 increases, C_q grows exponentially, though the actual QN ringing increases only slightly. Why this is so is clear in Eq. (4.6). The exponential factor $e^{-(t-x-x_2+2)/2}$ does increase exponentially with x_2 (this is the increase that shows up in C_q)

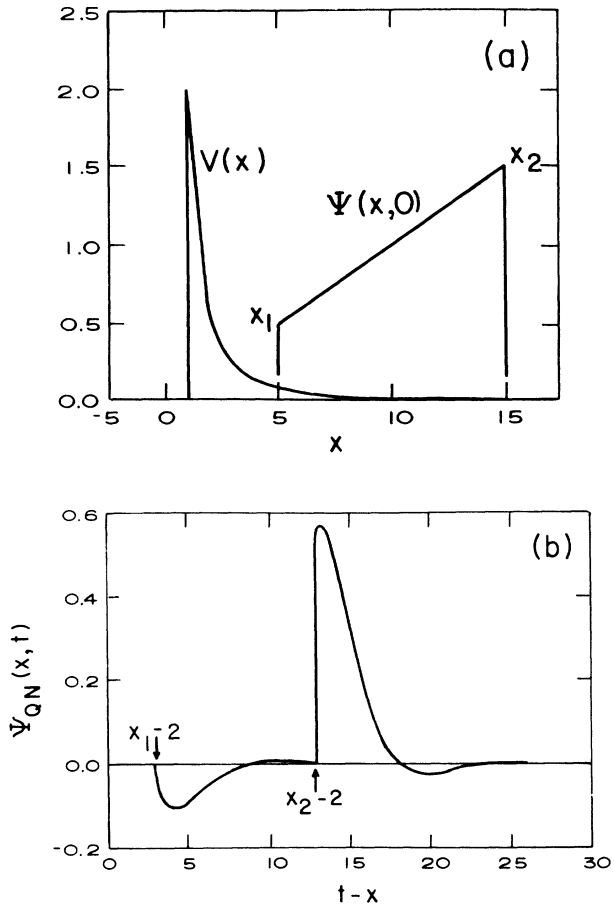

FIG. 6. Model problem showing two epochs of QN ringing. In (a) is shown the surrogate potential and the initial data. A waveform is shown in (b) of the resulting waveform. The curve shown corresponds to $x_1=5$ and $x_2=15$.

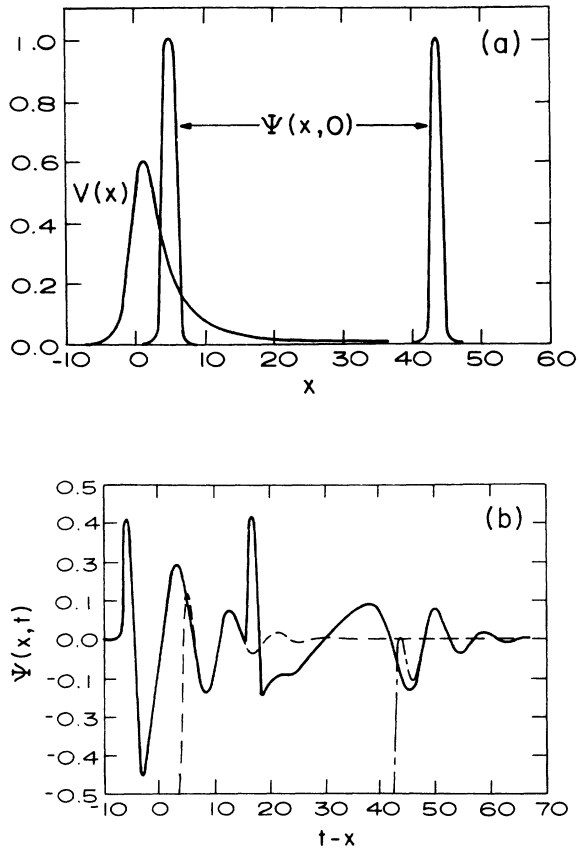

FIG. 7. Two epochs of quadrupole gravitational QN ringing in the Schwarzschild background. Initial data shown in (a) consist of Gaussian peaks at $r=4$ and 40, or $x=5.10$ and 43.66. The numerically evolved waveform, shown as the solid curve in (b), exhibits two epochs of QN ringing, starting at around $t-x\approx 5$ and 47. The other two curves show pure QN ringing (the superposition of the three least-damped QN quadrupole modes) with excitation coefficients computed separately for each bump.

but the step function that precedes the exponential guarantees that at the second turn on the argument of the exponential is zero. Timing prevents an exponential increase in the QN ringing. The small timing factor $e^{-(t-x+2)/2}$ cancels the large factor $e^{+x_2/2}$.

A numerical example shows that timing considerations for quadrupole gravitational QN ringing of a Schwarzschild hole [i.e., with the potential of Eq. (2.4)] are similar to those of the model problem. Initial data at $t=0$ are chosen to be $\partial\Psi/\partial t=0$ and

$$\Psi=\exp[-(r-4)^4]+\exp[-(r-40)^4]\ . \tag{4.8}$$

The results of numerical evolution of these initial data, presented in Fig. 7, show two apparent epochs of ringing. From the period and the decay rate of this ringing we find that each epoch is characterized by a complex frequency $s\approx -0.18-i0.75$, in good agreement with the QN frequency[13] $s_q=-0.177\,924\,6-i0.747\,343\,4$ for the least-damped quadrupole gravitational QN frequency for the Schwarzschild background. The times for the turn on of each epoch of ringing follow a pattern similar to that in the model problem above. Since wave propagation in the Schwarzschild background proceeds at $dx/dt=\pm 1$ we note that the peaks in the initial data at $r=4$ and 40, are, respectively, at $x=5.10$ and 43.66. The two epochs in Fig. 7 start at $t-x\approx 5$ and 47, which is consistent with the picture that the bumps propagate inward to the potential peak at $x\approx 0$ where they create the QN ringing.

Another interesting insight is to be found in this example. We can separate the initial data into two separate bumps at $r=4$ and 40, and can compute (for the mode with $s_q=-0.177\,924\,6-i0.747\,343\,4$) a separate excitation coefficient for each. [For the separate bumps or the combined bumps of Eq. (4.8) the excitation coefficient can be evaluated directly from Eq. (2.16).] The results are

single bump at $r=4$	$C_q=-0.485\,48-i0.014\,623$
single bump at $r=40$	$C_q=371.27-i109.38$
combined bumps	$C_q=370.78-i109.39$

(4.9)

Figure 7 shows the QN waveforms corresponding to each

of the two single-bump excitation coefficients above. The comparison with the numerically evolved data confirms that the two excitation coefficients give a reasonably accurate description of each epoch of ringing.

Note in Fig. 7 that the two epochs of ringing contain, to order of magnitude, the same amount of energy, but the excitation coefficient for the second epoch is larger than that for the first by a very large factor. Ths shows, as did the model problem with the surrogate potential, that Cauchy data far from the horizon can produce an enormous and misleading value of C_q. If the only source of QN ringing is a bump or edge far from the horizon, this presents no real problem; the large value of C_q is combined with the late turn-on time and results in a good estimate of the energy in the QN ringing. The real problem occurs if the QN ringing is due to some feature of the Cauchy data close to the horizon, but the Cauchy data also contain a distant bump or edge. In this case the irrelevant distant feature will dominate the value of C_q and make it useless for estimating the QN energy. The two methods found for dealing with this difficulty are described below.

B. Hand-shaped initial data

The simplest way to avoid difficulties with irrelevant Cauchy data at $x \gg 1$ (or, for that matter, at $x \ll -1$) is to eliminate that Cauchy data. We can keep only the Cauchy data in the neighborhood of $x \approx 0$. In doing this, however, we must be somewhat careful about the manner in which we truncate the data. If, for example, we replaced the actual Cauchy data, with data cut off sharply at some intermediate value of x, the sharp edge induced by the cut would itself generate QN ringing and would change C_q. The Cauchy data near $x \approx 0$ must be terminated smoothly. But, if the excitation coefficient depends delicately on the details of a smooth termination, this approach would not be very useful. Fortunately there is no such sensitivity.

As an example we consider quadrupole gravitational perturbations of a Schwarzschild hole with $\partial\Psi/\partial t = 0$ at $t = 0$. We suppose that Ψ at $t = 0$ has the form

$$\Psi = \frac{r-1}{r^2} + \text{“small bump at large } r \text{ .”} \tag{4.10}$$

The excitation coefficient due only to the $(r-1)/r^2$ part of the initial data is

$$C_q = -0.119\,58 + i0.068\,607 \tag{4.11}$$

for the QN mode at $s_q = -0.177\,924\,6 - i0.747\,343\,4$, and this value of C_q accurately describes the QN ringing that is excited by the initial data. If there were a small bump at large r there would be little change in the energy of the ringing, but the value of C_q would change significantly. To avoid the bump, and other distant features of the Cauchy data, we can terminate the Cauchy data at $r = r_0$, where r_0 is some moderately large value of r. We can then join the Cauchy data for $r < r_0$ to a tail of the form r^{-n} for $r > r_0$. Specifically, we replace the actual initial data by

$$\Psi(r, t=0) = \begin{cases} (r-1)/r^2, & r < r_0 , \\ \left[\dfrac{r_0 - 1}{r_0^2}\right]\left[\dfrac{r_0}{r}\right]^n, & r > r_0 . \end{cases} \tag{4.12}$$

For the choice $r_0 = 10$ the values of the excitation coefficient for various values of n are

n	C_q
0	$-0.116\,720 + i0.058\,114$
1	$-0.120\,849 + i0.086\,329$
2	$-0.122\,157 + i0.114\,470$
5	$-0.113\,086 + i0.191\,401$
10	$-0.080\,943 + i0.224\,837$
20	$-0.047\,185 + i0.230\,284$
∞	$-0.031\,409 + i0.232\,277$

(4.13)

For reasonably small values of n, the data are terminated gradually; for large values of n the termination is abrupt and, like a sharp turn off, this influences C_q. The division between gradual and abrupt termination can be understood quantitatively. Note that the characteristic length scale, $\lambda = \Psi/(\partial\Psi/\partial r)$, with which Ψ dies out is $\lambda \sim r_0/n$ at $r = r_0$. For n less than or of order 10, λ is larger than unity, i.e., larger than the Schwarzschild radius, and the termination is gradual; little QN ringing is excited. This is consistent with the fact that the values of C_q computed for $0 \le n < 5$ are all fairly close to each other, and are reasonably close to the value in Eq. (4.11). For $n \ge 10$, however, λ is smaller than unity and C_q is affected. The values of C_q for $n \ge 20$ vary very little and are all nearly equal to the value for $n = \infty$, i.e., for an abrupt turn off of the initial data.

The conclusion is clear: We may replace the actual Cauchy data with “hand-shaped” modified data. If we see to it that the length scale for termination of the Cauchy data is much larger than unity, the modified C_q computed will give a good estimate of the amount of QN ringing that will actually be excited by the original data.

C. Truncated expansion

The excitation at early time can be extracted from the Cauchy data through the use of a power-series expansion in the integrand for C_q. We start with the expression for $f_1(x,s)$ in Eq. (2.22), with s in the RHP so that the integrals exist, and we define

$$\begin{aligned} g_L(x,s) &\equiv y_L(x,s) S(x,s) e^{-xs} , \\ g_R(x,s) &\equiv A_{\text{out}}(s) y_R(x,s) S(x,s) e^{xs} . \end{aligned} \tag{4.14}$$

The factors $e^{\pm sx}$ on the right-hand side cancel the asymptotic behavior of y_L and y_R. For $S(x,s)$ well behaved at $|x| \to \pm\infty$, the functions g_L, g_R will also be asymptotically well behaved.

With g_L and g_R we now write Eq. (2.22) in terms of an arbitrary parameter s_0 as

$$f_1(x,s)=\int_{-\infty}^{x} g_L(x',s)e^{sx'}dx'+\int_{x}^{\infty} g_R(x',s)e^{-sx'}dx'$$
$$=\int_{-\infty}^{x} g_L(x',s)e^{(s+s_0)x'}e^{-s_0x'}dx'$$
$$+\int_{x}^{\infty} g_R(x',s)e^{-(s+s_0)x'}e^{s_0x'}dx' . \quad (4.15)$$

The expansions

$$e^{\pm(s+s_0)x'}=\sum_{n=0}^{\infty}\frac{(s+s_0)^n}{n!}(\pm x')^n$$

are then used to reexpress Eq. (4.15) as

$$f_1(x,s)=\sum_{n=0}^{\infty}\frac{(s+s_0)^n}{n!}\left[\int_{-\infty}^{x} g_L(x',s)(x')^n e^{-s_0x'}dx'+\int_{x}^{\infty} g_R(x',s)(-x')^n e^{s_0x'}dx'\right] . \quad (4.16)$$

In interchanging the summation and integration we have assumed that $\mathrm{Re}(s_0)<0$ and that, as a consequence, all the integrals in Eq. (4.16) exist.

To understand the convergence of the series we note that for large n the factor $x'^n e^{s_0x'}$ in the second integrand has a magnitude that peaks fairly sharply at $x\equiv x_n=n/\mathrm{Re}(-s_0)$, with a characteristic width of order $\Delta x\approx\sqrt{n}/\mathrm{Re}(-s_0)$. If, over this width, g_R is constant to order of magnitude and if $x\ll x_n$, we can approximate

$$\int_{x}^{\infty} g_R(x',s)x'^n e^{s_0x'}dx'\approx g_R(x_n,s)\int_{0}^{\infty} x'^n e^{s_0x'}dx'=g_R(x_n,s)\frac{n!}{s_0^{n+1}} . \quad (4.17)$$

The behavior of the first integral is similar. With these approximations the ratio of successive terms in the series $f_1(x,s)=\sum a_n$ is

$$\left|\frac{a_{n+1}}{a_n}\right|=\left|\frac{s+s_0}{s_0}\right|\left|\frac{g(x_{n+1},s)}{g(x_n,s)}\right| , \quad (4.18)$$

in which g represents g_L or g_R. As $n\to\infty$ the ratio $|g(x_{n+1},s)/g(x_n,s)|$ approaches unity unless the source function $S(x,s)$ asymptotically decreases exponentially or faster, in which case the ratio is less than unity. In any case a sufficient condition for convergence of the series is

$$\left|\frac{s+s_0}{s_0}\right|<1 . \quad (4.19)$$

The series in Eq. (4.16) was derived assuming that $\mathrm{Re}(s)>0$, but the convergence of the resulting series requires only the condition in Eq. (4.19); $\mathrm{Re}(s)$ can be positive or negative. The series, with the convergence condition of Eq. (4.19) satisfied, then gives an analytic continuation of $f_1(x,s)$ to values of s in the LHP and hence to the QN values of s. The terms in this series furthermore, have a very useful feature: In the second integral in Eq. (4.16) the Cauchy data are weighted with a function, $x^n e^{s_0x}$ that peaks fairly sharply at $x\equiv x_n=n/\mathrm{Re}(-s_0)$. Cauchy data far from the horizon will therefore not affect the low-n terms in the series. If the series seems to be converging after a few terms it can be truncated to give an answer for C_q untainted by any feature of the Cauchy data which will excite a later epoch of QN ringing.

To illustrate this we consider the Cauchy data at $t=0$ to be $\partial\Psi/\partial t=0$ and

$$\Psi=1/r^2+e^{-(r-40)^4} , \quad (4.20)$$

in which the second term adds a narrow "bump" at $r=40$ or $x\approx 44$ to the $1/r^2$ data which will turn on the early ringing. It is straightforward to compute, e.g., by contour deformation, the excitation coefficient for the Cauchy data in Eq. (4.20), as well as separate excitation coefficients for the $1/r^2$ part and for the $e^{-(r-40)^4}$ part [which was already given in Eq. (4.9)]. For the least-damped quadrupole Schwarzschild mode, the results are

$$C_q(1/r^2)=-0.200\,26+i0.042\,236 ,$$
$$C_q(\mathrm{bump})=371.27-i109.38 , \quad (4.21)$$
$$C_q(\mathrm{total})=371.07-i109.34 .$$

Results for C_q were also evaluated using the series in Eq. (4.16) with $s=s_q=-0.177\,924\,6-i0.747\,343\,4$, the value of the least-damped quadrupole QN frequency, and with $s_0=-0.5035+i0.949$. For this choice of s_0 the value of $\mathrm{Re}(-s_0)$ is large enough so that the integrals in Eq. (4.16) are easily evaluated to good accuracy, while at the same time $|(s_q+s_0)/s_0|$ is small enough so that the series converges fairly rapidly. In Fig. 8 the partial sums

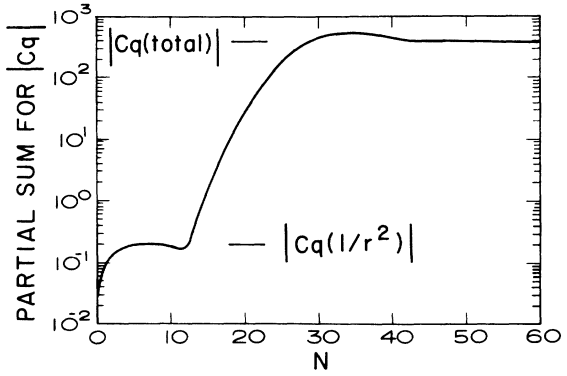

FIG. 8. The evaluation of C_q by a truncated series. The initial data is $\Psi=1/r^2+e^{-(r-40)^4}$, and C_q is evaluated as the sum $\sum a_n$, up to $n=N$, of the series expansion presented in the text. The magnitude of the partial sum evaluation is shown as a function of N. Also indicated are the values of $|C_q|$, computed by contour deformation, for the total Cauchy data and for the $1/r^2$ part alone.

of the series for C_q are shown as a function of N, the order of the highest term included. The series converges to $C_q(1/r^2)$ after only a few terms. As more terms are included the influence of the distant bump appears around $N \approx 14$ and the partial sum begins to evolve to C_q(total). The approximations for x_n and Δx which lead to Eq. (4.17), along with the fact that the bump is sharply peaked at $x \approx 44$, suggest that the bump will influence terms in the series from $n \approx 18$ to 27. In view of the approximate nature of the analysis, these values are in good agreement with the evolution shown in Fig. 8.

The applicability of the method of truncated expansion depends on the fact that within the Cauchy data there are two or more distinct features which turn on QN ringing and that these features are well separated. If, for example, the bump in our numerical example were located at $r=5$ rather than at $r=40$, the method would fail; for a bump at $r=10$ the method would work only marginally. The method of hand shaping the data similarly fails when the distinction is not clear between the two features of the Cauchy data which excite ringing. This inability to compute a value of C_q for the initial ringing is related to the fact that there is no well-defined initial ringing. There can be clearly defined first, second, and subsequent excitations of the QN ringing only if those excitations are separated by times significantly larger than the QN period. [For the least-damped quadrupole mode the QN period is $2\pi/|\mathrm{Im}(s_0)| = 8.4$.] If this condition is not satisfied the direct outward radiation of the Cauchy data will be similar in frequency to QN ringing. The identification of QN ringing will be meaningful only after the direct radiation has died off, only one epoch of QN ringing will appear, and only one C_q will be needed.

ACKNOWLEDGMENTS

The authors are grateful to Edward Leaver for useful discussions and for making available some of his numerical results and computer programs. This research was supported in part by the National Science Foundation under Grant No. PHY-8503653.

[1]Kip S. Thorne, in *Three Hundred Years of Gravitation*, edited by S. W. Hawking and W. Israel (Cambridge University Press, Cambridge, England, 1987).
[2]C. V. Vishveshwara, Nature (London) **227**, 937 (1970).
[3]W. H. Press, Astrophys. J. Lett. **170**, L105 (1971); see also C. J. Goebel, *ibid.* **172**, L95 (1972).
[4]S. L. Detweiler and E. Szedenits, Astrophys. J. **231**, 211 (1979).
[5]S. Detweiler, Proc. R. Soc. London **A352**, 381 (1977).
[6]C. T. Cunningham, R. H. Price, and V. Moncrief, Astrophys. J. **224**, 643 (1978).
[7]C. T. Cunningham, R. H. Price, and V. Moncrief, Astrophys. J. **230**, 870 (1979).
[8]C. T. Cunningham, R. H. Price, and V. Moncrief, Astrophys. J. **236**, 674 (1980).
[9]L. Smarr, in *Sources of Gravitational Radiation*, edited by L. Smarr (Cambridge University Press, Cambridge, England, 1979).
[10]R. F. Stark and T. Piran, Phys. Rev. Lett. **55**, 891 (1985); **56**, 97(E) (1986).
[11]S. Chandrasekhar and S. Detweiler, Proc. R. Soc. London **A344**, 441 (1975).
[12]S. Detweiler, Astrophys. J. **239**, 292 (1980).
[13]E. W. Leaver, Proc. R. Soc. London **A402**, 285 (1985).
[14]V. Ferrari and B. Mashhoon, Phys. Rev. D **30**, 295 (1984); V. Ferrari and B. Mashhoon, Phys. Rev. Lett. **52**, 1361 (1984).
[15]S. Iyer and C. M. Will, Phys. Rev. D **35**, 3621 (1987); S. Iyer, *ibid.* **35**, 3632 (1987).
[16]E. W. Leaver, Phys. Rev. D **34**, 384 (1986).
[17]C. W. Misner, K. S. Thorne, and J. A. Wheeler, *Gravitation* (Freeman, San Francisco, 1973).
[18]This result and the contour in Fig. 5 bear a strong resemblance to the approach illustrated in Fig. 3 of Ref. 16. In that work, however, it was not shown that the contour deformation is equivalent to analytic continuation. Furthermore, the leading factor on the right in Eq. (3.10), $[1-\exp(2\pi i s_q)]^{-1}$, is missing in Ref. 16.
[19]R. H. Price, Phys. Rev. D **5**, 2419 (1972).